Excitation of localized surface plasmon resonance using a core–shell structured nanoparticle layer substrate and its application for label-free detection of biomolecular interactions

2007 J. Phys.: Condens. Matter 19 215201

(http://iopscience.iop.org/0953-8984/19/21/215201)

IOP PUBLISHING JOURNAL OF PHYSICS: CONDENSED MATTER

J. Phys.: Condens. Matter **19** (2007) 215201 (10pp) doi:10.1088/0953-8984/19/21/215201

Excitation of localized surface plasmon resonance using a core–shell structured nanoparticle layer substrate and its application for label-free detection of biomolecular interactions

Tatsuro Endo[1], Kagan Kerman[2], Naoki Nagatani[3] and Eiichi Tamiya[2,4]

[1] Department of Mechano-Micro Engineering, Interdisciplinary Graduate School of Science and Engineering, Tokyo Institute of Technology, 4259 Nagatsuta-cho, Midori-ku, Yokohama 226-8502, Japan
[2] School of Materials Science, Japan Advanced Institute of Science and Technology (JAIST), 1-1 Asahidai, Nomi City, Ishikawa 923-1292, Japan
[3] Department of Biotechnology and Applied Chemistry, Faculty of Engineering, Okayama University of Science, 1-1 Ridai-cho, Okayama 700-0005, Japan

E-mail: jaist-tamiya@jaist.ac.jp

Received 23 August 2006
Published 1 May 2007
Online at stacks.iop.org/JPhysCM/19/215201

Abstract

The novel characteristics of nanomaterials enable highly sensitive and specific applications in electronics, optics and biotechnology. In particular, nanomaterials have become the preferable tools for monitoring biomolecular interactions on a biochip without labelling procedures using enzymes and fluorescent dyes. In this report, label-free detection of hybridization between nucleic acids using localized surface plasmon resonance (LSPR) based on a core–shell structured nanoparticle layer substrate is described. The core–shell structured nanoparticle layer substrate could be excited using LSPR phenomena, and its LSPR characteristics were controlled by applying different fabrication conditions. Using our LSPR label-free biochip, the optical characteristics were monitored for the detection of specific DNA–DNA and PNA–DNA hybridization reactions. Furthermore, the detection limit of the LSPR label-free biochip was 1 pM. The highly sensitive label-free detection of DNA hybridization was possible in a short analysis time. As a result, the LSPR label-free biochip provides a promising platform with attractive advantages for the detection of biomolecular interactions at low cost in a simplified experimental set-up with a low sample volume.

[4] Author to whom any correspondence should be addressed.

1. Introduction

Unravelling the secrets behind the biomolecular interactions between nucleic acids and proteins has been the paramount research topic of all times. To understand the mechanism and the main role players in these interactions, numerous bioassay systems have been developed in the past decades. In particular, well-established systems, such as enzyme-linked immunosorbent assay (ELISA) [1–3], two-dimensional (2D) electrophoresis [4, 5] and polymerase chain reaction (PCR) [6, 7], have become indispensable methods in life sciences. However, these conventional bioassays bring with them several disadvantages during the experimental process, such as high sample volumes, troublesome liquid handling and problems in time management. To improve these disadvantages, an intensive amount of research has been focused on the bio-microelectromechanical system (bioMEMS), the micro-total analysis system (μ-TAS) and Lab-on a chip (LOC) [8–10]. These biochips allow the interaction of biomolecules in a well-controlled and small area. Therefore, the disadvantages of the conventional bioassays have been greatly improved [11–14]. The biochips rely on several detection principles for the biomolecular interactions, such as optics [15], electrochemistry [16, 17] and so on. However, these detection principles mostly require a labelling procedure using enzymes and fluorescent dyes. The labelling procedure causes degradation in the recognition ability of the biomolecules, which may lead to problems in the binding efficiency.

An alternative way of detecting the biomolecules without disrupting their natural states and functions has been in great demand. Thus, a new wave of sensing technology was created; 'label-free' technology provided optical, electrochemical, piezoelectric and other detection possibilities, in which the biomolecules did not have to be attached to a 'label'. Several kinds of label-free biochips based on surface plasmon resonance (SPR) [18] and quartz crystal microbalance (QCM) [19] have been developed. Unfortunately, these label-free biochips had their own disadvantages, such as highly sophisticated apparatus, high cost, and so on. However, it still remains a fact that label-free biochips have a high possibility of realizing more convenient bioassay systems than conventional ones. If the development of label-free biochips progresses in parallel to the great demand, they may soon become an important part of routine analysis in various fields.

To develop more convenient label-free biochips, we focused on the use of nanostructured materials. Recently, the characteristics of nanomaterials have been studied in detail theoretically, and these characteristics have been applied in several fields. Nanomaterials have unique physical and chemical characteristics due to their quantum size effects. Based on these characteristics, nanomaterials were used as quantum dots (QDs) and metal nanoparticles, such as gold colloids. If these interesting characteristics of nanomaterials could be applied for the label-free detection of biomolecular interactions, more convenient label-free biochips would be established. Therefore, we aimed to develop a localized surface plasmon resonance (LSPR) based label-free biochip.

LSPR is well known to be excited on nanostructured noble metals, such as gold, platinum and copper. Noble metals have intrigued people for centuries because of their optical properties, glowing brightly in various attractive colours. These properties are strongly dependent on the size, shape, and the local environment of the metal nanostructures, as described by Mie theory [20–22]. Briefly, as the size of a metal structure decreases from the bulk-scale (m to μm) to the nano-scale ($<$100 nm), the movement of electrons through the internal metal framework becomes restricted. As a result, metal nanoparticles display specific extinction bands in the UV–visual spectra, when the incident light resonates with the conduction band electrons at their surfaces. These charge density oscillations are simply defined as the LSPR.

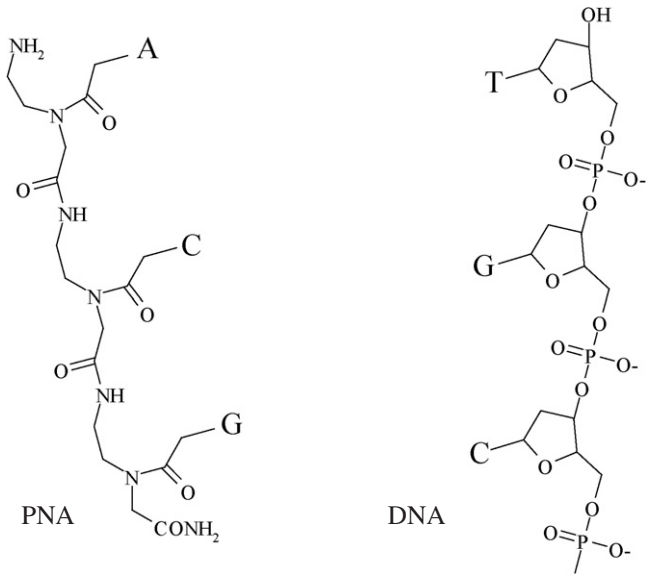

Figure 1. Chemical structures of PNA and DNA.

In the last five years, numerous reports about LSPR label-free biochips using metal nanoparticles have been presented [23–29]. However, controlling the diameter and the shape of the metal nanoparticles has always been a difficult task. Furthermore, the attachment of the metal nanoparticles and the control of their density on the chip surface requires sophisticated fabrication techniques. In order to overcome these problems of conventional LSPR-based biochips, we fabricated a core–shell structured nanoparticle layer substrate for the excitation of the LSPR on its surface [30, 31]. This substrate consisted of dielectric nanoparticles and metal layers that surrounded these dielectric nanoparticles. The core–shell structured nanoparticle layer substrate displayed the excitation of the LSPR, and its optical characteristics could be controlled by the fabrication conditions, such as the nanoparticle diameter and the thickness of the metal layers. The optical characteristics of the LSPR label-free biochips using noble metal nanoparticles or metal nanoislands, such as gold and silver, were commonly detected with the help of a shift in the absorbance peak wavelength. However, the increase in the intensity at the peak wavelength along with the increasing layer thickness was reported previously [32, 33]. Similarly, we could observe a significant increase in the absorbance intensity using our gold-capped nanoparticle layer of the LSPR label-free biochip.

In this research, peptide nucleic acids (PNAs) and DNA were used as the biorecognition layers on our LSPR label-free biochip. PNAs are neutral and achiral DNA mimics with a pseudopeptide backbone. PNA is an extremely good structural mimic of DNA (figure 1), and PNA oligomers are able to form stable duplex structures with Watson–Crick complementary DNA and RNA oligomers. With its exceptional structure, PNA has major applications as a tool in molecular biology and biochip applications. A PNA probe was designed to recognize the target DNA, which was related to a mutation in tumour necrosis factor (TNF-α). TNF-α is a pleiotropic inflammatory cytokine. Additionally, TNF-α is a central hallmark of inflammation and the basis of oedema in many acute and chronic disease states, including ischaemia and reperfusion injury. The single-nucleotide polymorphisms (SNPs) from G to A at position -308 within the TNF-α promoter were reported to affect the capacity to secrete TNF-α in response to endogenous (e.g., cytokines) or exogenous stimuli (e.g., lipopolysaccharides). In the following

sections, we report on the characteristics of the hybridization reactions that were monitored between DNA and PNA oligomers immobilized on the LSPR label-free biochip surfaces.

2. Experimental details

2.1. Reagents and apparatus

A self-assembled monolayer (SAM) on the gold substrate surface was formed using 4,4′-dithiodibutyric acid (DDA) as supplied by Aldrich. 1-ethyl-3-(3-dimethylaminopropyl) carbodiimide (EDC) for activation of the carboxyl group of DDA was purchased from Dojindo Laboratories (Kumamoto, Japan). The surface of the silica nanoparticles was modified using 3-aminopropyltriethoxysilane (γ-APTES) as purchased from Shin-Etsu Chemical Co., Ltd (Tokyo, Japan). Silica nanoparticles (particle diameter: 100 nm) for preparing the nanoparticle layer were purchased from Polysciences Inc. (Warrington, PA). Slide glass substrates (S-1111, 76 × 26 mm, thickness: 0.8–1.0 mm) were purchased from Matsunami Glass Ind., Ltd (Osaka, Japan). *N*-hydroxysuccinimide (NHS) and streptavidin for PNA or DNA probe immobilization were purchased from Wako Pure Chemical Industries, Ltd (Osaka, Japan). PNA and DNA probes, target DNA and single-base mismatch DNA were obtained from Fasmac (Kagawa, Japan). Ultra-pure water (18.3 MΩ cm) from Millipore was used in all preparations.

For the deposition of chromium and gold layers on the slide glass substrate surface, a thermal evaporator (SVC-700TM/700-2) was purchased from Sanyu Electron Co., Ltd (Tokyo, Japan). For monitoring of the base pressure, an analogue ionization vacuum gauge was utilized (GI-TL3, Ulvac, Kanagawa, Japan). The growth rate in thickness was monitored by a quartz crystal microbalance (QCM, Model TM-200R, Maxtek Inc., CA, USA). The spectrophotometer (USB-2000 UV–vis, wavelength range: 200–1100 nm), tungsten halogen light source (LS-1, wavelength range: 360–2000 nm), and optical fibre probe bundle (R-200-7 UV–vis, fibre core diameter: 200 μm, wavelength range: 250–800 nm) were purchased from Ocean Optics (Dunedin, USA).

2.2. Fabrication of LSPR label-free biochip

For the fabrication of the LSPR label-free biochip, the surface modified silica nanoparticles were attached onto the gold deposited glass substrate surface. The surface modification procedure was performed as described in our previous reports [30, 31]. After the surface modification, the surface modified silica nanoparticles were stored at room temperature (RT) until use.

To form the nanoparticle layer, the deposition of the chromium and gold bottom layer onto the slide glass substrate surface was carried out using thermal evaporator. The thermal evaporator was used at a base pressure of 3×10^{-6} Torr. The growth rate was monitored by the QCM, and was manually adjusted to 1.0 Å s^{-1}. Finally, slide glass substrates that were deposited with a 5.0 nm chromium layer and a 40 nm gold bottom layer were obtained. After the deposition of the chromium and gold layers on the slide glass substrate, the formation of the nanoparticle layer was carried out as reported previously [30, 31]. After the nanoparticle layer formation, 30 nm of the gold top layer was deposited using the thermal evaporator.

From these fabrication procedures, the specific excitation of the LSPR could be observed. Additionally, the optical characteristics of the LSPR label-free biochip could be controlled by changing the fabrication conditions, such as the nanoparticle layer condition and thickness of the gold layers. Furthermore, the optical characteristics of our LSPR label-free biochip were almost similar to the optical characteristics of the LSPR excited by using core–shell structured nanoparticles [32, 33].

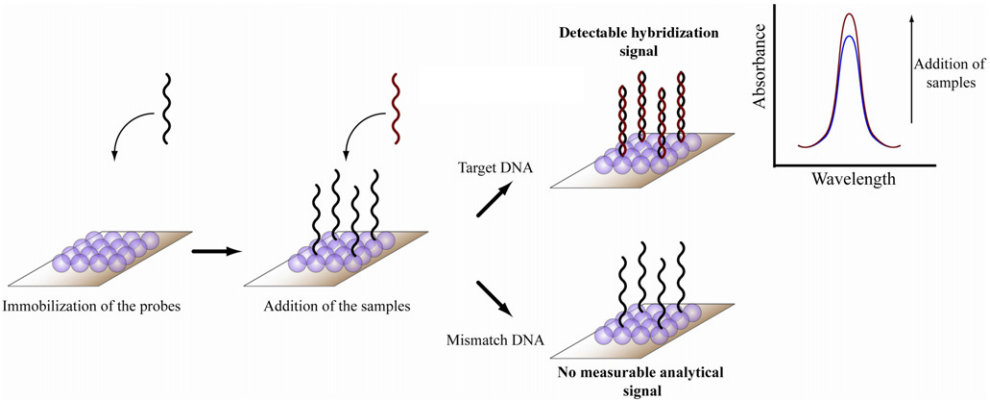

Figure 2. Experimental procedure using the LSPR label-free biochip.
(This figure is in colour only in the electronic version)

2.3. Label-free detection of the PNA–DNA or DNA–DNA hybridization using LSPR label-free biochip

Synthetic oligonucleotides were used for the label-free detection of PNA–DNA and DNA–DNA hybridization reactions, and they had the following sequences:

PNA and DNA probe:(5′)H–Biotin–ACC ACC ACT TC–NH_2(3′).

DNA target:5′–GGT TTC GAA GTG GTG GTC TTG–3′

Single-base mismatch target:5′–GGT TTC GAA GCG GTG GTC TTG–3′.

For the label-free detection of PNA–DNA or DNA–DNA hybridization, target DNA solutions at different concentrations (5.0 μl, 0–1.0 μM) were introduced to PNA or DNA probes immobilized on the LSPR optical biochip surface, and left for hybridization at RT in 10 min. As a control experiment, an excess amount of (1.0 μM) single-base mismatch target DNA solution was introduced, and kept for 10 min. After a stringent washing procedure with 1% (v/v) Tween-20, the change in the absorption spectrum caused by the hybridization was observed.

The experimental procedure for the optical characteristics evaluation used in this research is shown in figure 2. All absorbance spectra were monitored from 400 to 800 nm on the UV–vis spectrophotometer at RT. White light emerging from the optical fibre bundle was incident onto the core–shell structured nanoparticle layer substrate from the vertical direction. The reflected light was coupled with the detection fibre probe of the optical fibre bundle and analysed using the UV–vis spectrophotometer.

3. Results and discussion

3.1. Evaluation of the probe immobilization efficiency on the LSPR label-free biochip surface

First, the optimization of the probe immobilization conditions, such as concentration, and immobilization time, were carried out. In the experiment, PNA or DNA probe solutions at different concentrations (1 pM–1 μM) were introduced onto the biochip surface. Additionally, probe immobilization at different immobilization time periods was carried out. After the immobilization, the optical characterization of the probe immobilized LSPR label-free biochip was carried out.

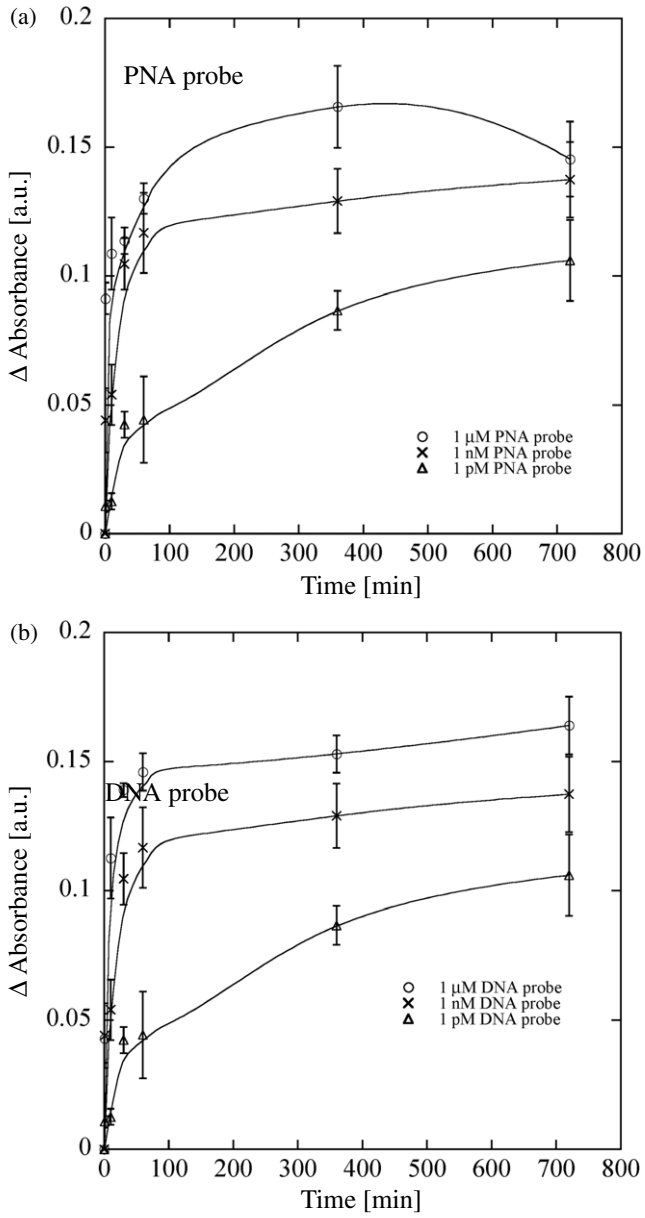

Figure 3. Time dependence of the probe immobilization onto LSPR label-free biochip surface.

The time dependence of PNA probe (figure 3(a)) and DNA probe (figure 3(b)) immobilization at different concentrations is shown in figure 3. Changes in the intensity of the LSPR signals with immobilization time could be observed. However, the signals did not change significantly after an immobilization time of over 1 h. Thus, 1 h was employed as the optimum probe immobilization time. The concentration dependence of the LSPR signals was also observed. The LSPR signals were greatly affected by the probe concentration, and the absorbance intensity saturated over 1 h. From these immobilization characteristics, probe immobilization onto the LSPR label-free biochip surface was carried out using a 1 μM PNA or

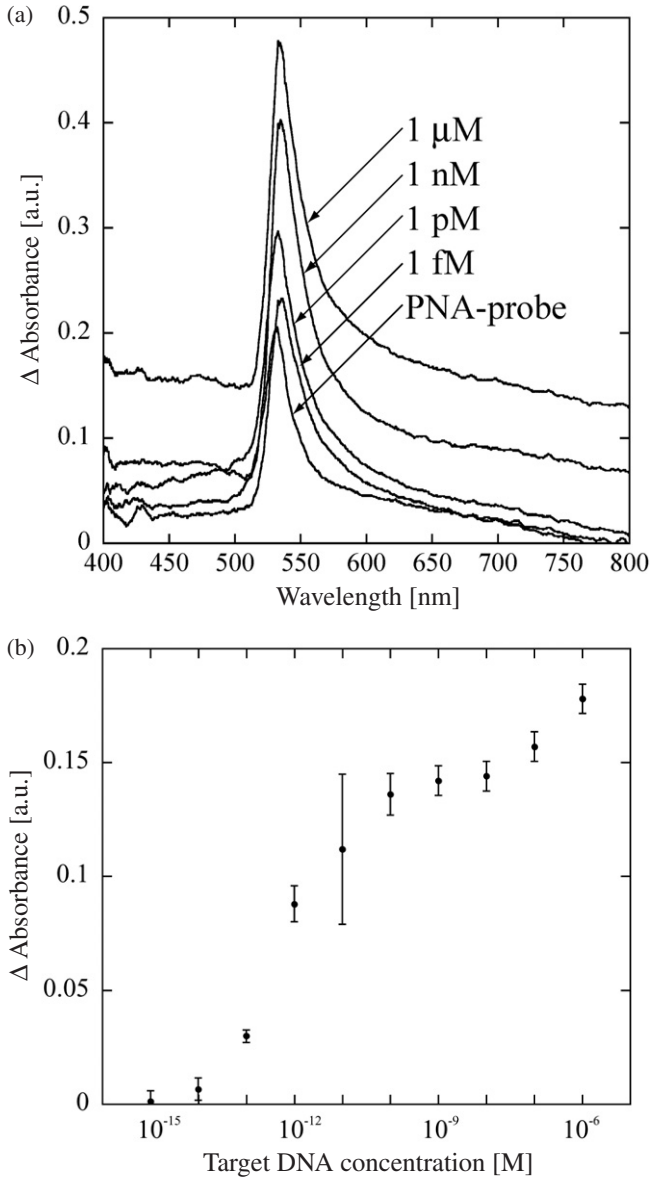

Figure 4. Optical characteristics and calibration curve using the PNA probe immobilized LSPR label-free biochip.

DNA probe for 1 h. After probe immobilization under these optimum conditions, the label-free detection of hybridization reactions was performed.

3.2. Label-free detection of the PNA–DNA and DNA–DNA hybridization reactions

We recorded the changes in the absorbance strength after the introduction of target DNA molecules at different concentrations. Using our LSPR label-free biochip, the peak absorbance wavelength of the core–shell structured nanoparticle layer substrate was observed at 536 nm. The optical characteristics evaluation of DNA hybridization was carried out using PNA (figure 4) and DNA (figure 5) probe immobilized LSPR label-free biochips. As a result, a sharp

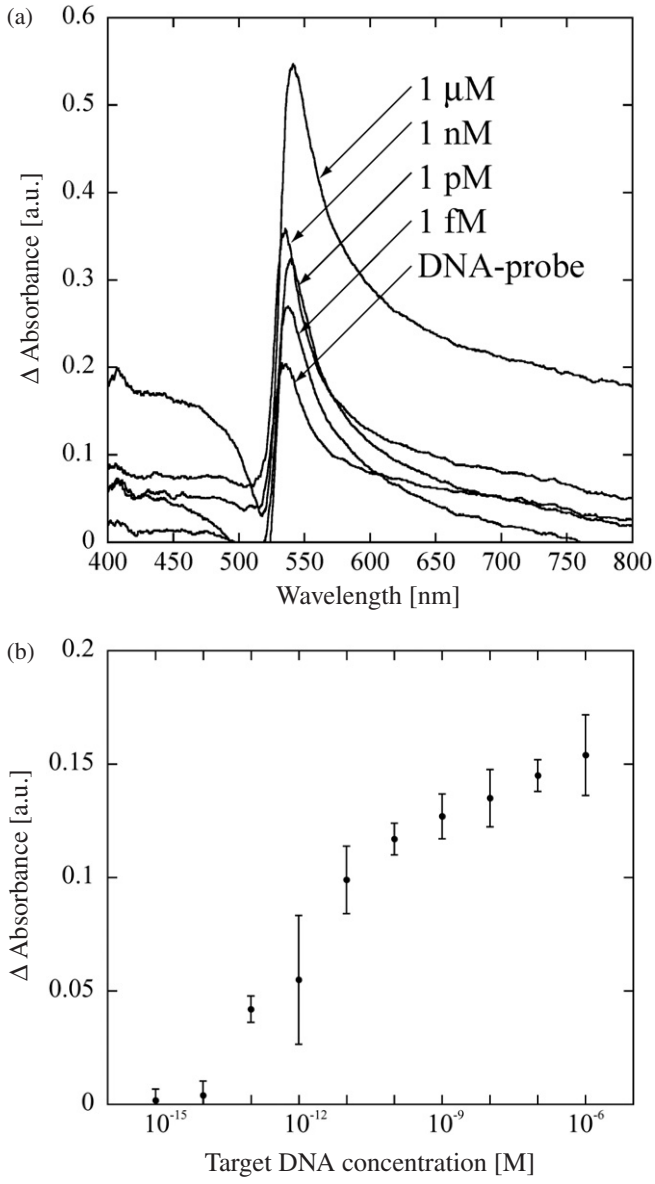

Figure 5. Optical characteristics and calibration curve using the DNA probe immobilized LSPR label-free biochip.

increase in the LSPR signals in relation to the target DNA concentration could be observed at the PNA probe immobilized biochip (figure 4(a)) and the DNA probe immobilized biochip (figure 5(a)). The detection limit of our biochip was calculated from three times the standard deviation divided by the slope of the calibration curve. From these calculation results, we determined that the detection limit of the PNA probe immobilized biochip was 0.677 pM target DNA (figure 4(b)). Accordingly, the detection limit of the DNA probe immobilized biochip was 0.803 pM target DNA (figure 5(b)).

The discrimination against a single-base mismatch was also achieved by using both PNA and DNA probe immobilized LSPR label-free biochips. When an excess amount of single-base mismatch target DNA at 1.0 μM was introduced onto the PNA or DNA probe immobilized

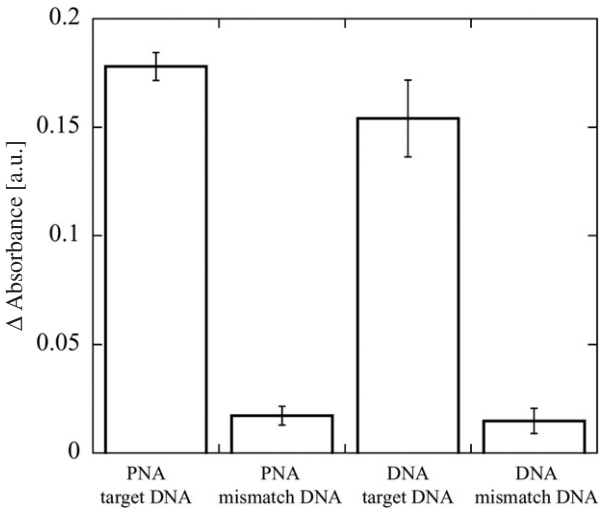

Figure 6. Absorbance strength change after the introduction of 1 μM target DNA or mismatch DNA onto the PNA or DNA probe immobilized LSPR label-free biochip surface.

LSPR label-free biochip, no LSPR signal change was observed in either of the biochips (figure 6). We concluded that the non-specific adsorption could be suppressed by the stringent washing of the biochip surface, as described in section 2.

In addition, the variation in the LSPR signals was compared between PNA and DNA probes from the calibration characteristics. The variation of absorbance intensity with PNA probes was smaller than that obtained from DNA probes. Since DNA is negatively charged, repulsion occurs between two complementary strands. On the other hand, PNA is a neutral and chemically stable molecule. The hybrids of PNA with DNA or RNA sequences generally show thermal stabilities higher than the corresponding DNA–DNA or DNA–RNA duplexes. Therefore, we could monitor hybridization reactions using PNA probes with narrow relative standard deviation (RSD) results.

4. Conclusions

In this research, an LSPR label-free biochip constructed with a core–shell structured nanoparticle layer substrate was applied for the label-free detection of PNA–DNA and DNA–DNA hybridization reactions. PNA and DNA probe immobilized LSPR label-free biochips are promising candidates for the specific detection of target DNA. The LSPR label-free biochip is easy to fabricate, and the apparatus cost for the optical characteristics evaluation is significantly lower than that of a conventional SPR apparatus; also, the operation procedure has become more convenient, without any labelling procedures. Moreover, the core–shell structured nanoparticle layer substrate could detect low concentrations of target DNA. From these advantages, we concluded that the novel characteristics of our substrate that could excite LSPR is more suitable for monitoring biomolecular interactions than the conventional LSPR-based biochips reported previously. Certainly, the LSPR-based label-free optical monitoring method promises to offer a massively parallel detection capability in a highly miniaturized package.

Acknowledgments

The authors wish to thank Dr Masato Saito from the Japan Advanced Institute of Science and Technology (JAIST), for valuable advice during the detection of PNA–DNA and DNA–DNA hybridization reactions using the LSPR label-free biochip. The authors also would like to thank Drs Yasuko Yanagida and Takeshi Hatsuzawa from the Tokyo Institute of Technology for a critical reading of our manuscript.

References

[1] Yang X-X, Hu Z-P, Chan S-Y and Zhou S-F 2006 *Clin. Chim. Acta* **365** 9
[2] Butler J E, McGivern P L and Swanson P 1978 *J. Immunol. Methods* **20** 365
[3] Wood D D, Gammon M and Staruch M J 1982 *J. Immunol. Methods* **26** 19
[4] Righetti P G 1990 *J. Chromatogr.* A **516** 3
[5] Chiou S-H and Wu S-H 1999 *Anal. Chim. Acta* **383** 47
[6] Johnson J R 2000 *J. Microbiol. Methods* **41** 201
[7] Knox C M, Chandler D, Short G A and Margolis T P 1998 *Ophthalmology* **105** 37
[8] Chován T and Guttman A 2002 *Trends Biotechnol.* **20** 116
[9] Lopez M F and Pluskal M G 2003 *J. Chromatogr.* B **787** 19
[10] Bashir R 2004 *Adv. Drug Deliv. Rev.* **56** 1565
[11] Endo T, Okuyama A, Matsubara Y, Nishi K, Kobayashi M, Yamamura S, Morita Y, Takamura Y, Mizukami H and Tamiya E 2005 *Anal. Chim. Acta* **531** 7
[12] Matsubara Y, Kerman K, Kobayashi M, Yamamura S, Morita Y and Tamiya E 2005 *Biosensors Bioelectron.* **20** 1482
[13] Matsubara Y, Kerman K, Kobayashi M, Yamamura S, Morita Y, Takamura Y and Tamiya E 2004 *Anal. Chem.* **76** 6434
[14] Mitsubayashi K, Wakabayashi Y, Tanimoto S, Murotomi D and Endo T 2003 *Biosensors Bioelectron.* **19** 67
[15] Murakami Y, Endo T, Yamamura S, Nagatani N, Takamura Y and Tamiya E 2004 *Anal. Biochem.* **334** 111
[16] Kerman K, Saito M, Morita Y, Takamura Y, Ozsoz M and Tamiya E 2004 *Anal. Chem.* **76** 1877
[17] Kerman K, Vestergaard M, Nagatani N, Takamura Y and Tamiya E 2006 *Anal. Chem.* **78** 2182
[18] Wilson P K, Jiang T, Minunni M E, Turner A P F and Mascini M 2005 *Biosensors Bioelectron.* **20** 2310
[19] Tombelli S, Minunni M, Luzi E and Mascini M 2005 *Bioelectrochemistry* **67** 135
[20] Jin R, Cao Y, Mirkin C A, Kelly K L, Schatz G C and Zheng J G 2001 *Science* **294** 1901
[21] Prasad N P 2004 *Nanophotonics* (New York: Wiley) pp 129–51
[22] Hutter E and Fendler J H 2004 *Adv. Mater.* **16** 1685
[23] Haes A J and Van Duyne R P 2004 *Anal. Bioanal. Chem.* **379** 920
[24] Nath N and Chilkoti A 2002 *Anal. Chem.* **74** 504
[25] Nath N and Chilkoti A 2004 *J. Fluoresc.* **14** 377
[26] Nath N and Chilkoti A 2004 *Anal. Chem.* **76** 5370
[27] Haes A J and Van Duyne R P 2002 *J. Am. Chem. Soc.* **124** 10596
[28] Riboh J C, Haes A J, McFarland A D, Yonzon C R and Van Duyne R P 2003 *J. Phys. Chem.* B **107** 1772
[29] Frederix F, Friedt J M, Choi K H, Laureyn W, Campitelli A, Mondelaers D, Maes G and Borghs G 2003 *Anal. Chem.* **75** 6894
[30] Endo T, Yamamura S, Nagatani N, Morita Y, Takamura Y and Tamiya E 2005 *Sci. Tech. Adv. Mater.* **6** 491
[31] Endo T, Kerman K, Nagatani N, Takamura Y and Tamiya E 2005 *Anal. Chem.* **77** 6976
[32] Liz-Mazran L M, Giersig M and Mulvaney P 1996 *Langmuir* **12** 4329
[33] Petit C, Lixon P and Pileni M P 1990 *J. Phys. Chem.* **94** 1598